Observation of all-in type tetrahedral displacements in nonmagnetic pyrochlore niobates

S. Torigoe,[1] Y. Ishimoto,[2] Y. Aoishi,[1] H. Murakawa,[1] D. Matsumura,[3] K. Yoshii,[3] Y. Yoneda,[3] Y. Nishihata,[3] K. Kodama,[4] K. Tomiyasu,[5] K. Ikeda,[6] H. Nakao,[6] Y. Nogami,[2] N. Ikeda,[2] T. Otomo,[6] and N. Hanasaki[1]

[1]*Department of Physics, Osaka University, Toyonaka, Osaka 560-0043, Japan*

[2]*Department of Physics, Okayama University, Tsushimanaka, Okayama 700-8530, Japan*

[3]*Synchrotron Radiation Research Center, Japan Atomic Energy Agency, Hyogo 679-5148, Japan*

[4]*Quantum Beam Science Directorate, Japan Atomic Energy Agency, Tokai, Ibaraki 319-1195, Japan*

[5]*Department of Physics, Tohoku University, Aoba, Sendai 980-8578, Japan*

[6]*Institute of Materials Structure Science, High Energy Accelerator Research Organization (KEK), oho, Tsukuba, Ibaraki 305-0801, Japan*

(Received 8 May 2015; revised manuscript received 28 December 2015; published 4 February 2016)

We observed all-in type Nb tetrahedral displacement in nonmagnetic pyrochlore niobates $A_2Nb_2O_7$ (A = $Nd_{0.5}Ca_{0.5}$ and $Y_{0.5}Ca_{0.5}$) through the analysis of the neutron pair distribution function and the extended x-ray absorption function spectroscopy. The all-in type Nb tetrahedral displacement, which has the character of a charge singlet state, is driven by the formation of the bonding orbital. The diffuse scattering in the x-ray diffraction, which has the resonant component in the Nb L_3 edge, indicates that the all-in type Nb tetrahedral displacement has the periodicity with its short-range correlation.

DOI: 10.1103/PhysRevB.93.085109

I. INTRODUCTION

Material with macroscopic entropy preserved by crystal geometry is one of the most interesting research objects in condensed matter physics. The most prototypical example is crystalline ice, in which the spatial configuration of two types of hydrogen-oxygen bonds of different length, i.e., a covalent bond and hydrogen bond, cannot be uniquely fixed [1]. Consequently, the significant amount of entropy induced by this degeneracy is not released. In this case, the hydrogen position deviates from the center of the bilateral oxygen and takes the so-called two-in two-out configuration in the corner-sharing tetrahedra. The corner-sharing tetrahedra formed by the middle point between the oxygens are regarded as the pyrochlore lattice. Here, the essential point to give rise to macroscopic entropy is the restricted distribution of the physical quantity with two types of freedom (e.g., in or out) on the tetrahedral corner in the pyrochlore lattice [2]. This concept can be applied to a magnetic system as represented by the f electron compounds $R_2Ti_2O_7$ (R = Dy and Ho) with magnetic frustration in the spin-ice state [3].

In d electron systems, it is expected that the orbital will be hybridized with the neighboring sites in the transition-metal tetrahedra, since the spread of the wave function is much larger than that of an f electron. The orbital hybridization modulates the highly symmetric lattice to form the ordered phase [4–6]. Its resultant atomic displacement and multimer formation have been reported for the d electron systems in several spinel compounds. For example, in AlV_2O_4, in which the valence of the V atoms is +2.5 ($3d^{2.5}$), the heptamer is formed in the V sites [5]. In $CuIr_2S_4$, in which the valence of the Ir atoms is +3.5 ($5d^{5.5}$), the octamer exists in the Ir sites [6]. These materials have the long-range order of the atomic displacements and the charge order, which releases geometrical frustration. Similar situations are also expected in pyrochlore oxides of the d electron system. An ideal (non-distorted) pyrochlore oxide $A_2B_2O_7$ belongs to the space group $Fd\bar{3}m$, and the lattice constant is ≈ 10 Å (e.g., the lattice constant is 10.365 Å in $Cd_2Nb_2O_7$ at room temperature) [7]. As shown in Fig. 1(a), the A-site and the B(Nb)-site atoms form the corner-sharing tetrahedra, respectively. Figure 1(b) shows the relative atomic positions around the Nb atom with oxygen octahedra, which is pointed out by the arrow in Fig. 1(a). The pyrochlore niobate $Y_2Nb_2O_7$ is the nonmagnetic insulator, though the average valence of the Nb atom is +4 ($4d^1$) [8]. In their theoretical study, Blaha *et al.* pointed out that the charge singlet state having the all-in type atomic displacement in Nb tetrahedra is the ground state [9]. McQueen *et al.* reported that the Nb atoms are displaced inward or outward in the Nb tetrahedra through the neutron powder diffraction in $(Y_{0.5}Ca_{0.5})_2Nb_2O_7$, as shown in Fig. 1(c) [10]. Unfortunately, the detailed Nb displacement pattern has not been revealed yet.

In this paper, we report the Nb tetrahedral displacement having the all-in type configuration experimentally. This Nb tetrahedral displacement has a periodicity with the short correlation length. We argue that the non-magnetic state and the charge disproportionation occur in the pyrochlore niobates.

II. EXPERIMENT

$A = Nd_{0.5}Ca_{0.5}$ and $Y_{0.5}Ca_{0.5}$ were synthesized under an Ar and H_2 atmosphere by the floating zone method [10,11]. The starting materials were Y_2O_3, Nd_2O_3, NbO_2, and $Ca_2Nb_2O_7$, the last of which was prepared by using $CaCO_3$ and Nb_2O_5 in air. The characterization of the samples was confirmed by x-ray diffraction, energy dispersive x-ray spectroscopy, and thermogravity.

The hard and soft x-ray diffraction were measured at BL-4C and BL-11B of the Photon Factory, respectively [12–14]. In the neutron pair distribution function (PDF) [6,15], the total scattering structure function $S(Q)$ and the PDF $G(r)$ were obtained at BL-21 of J-PARC (NOVA). The PDF $G(r)$ was obtained by the inverse Fourier transformation of the $S(Q)$ and analyzed using the PDFgui [16]. The x-ray absorption spectroscopy (XAS) data were gathered at BL-14B1 of SPring-8 [17]. The thickness of the samples was adjusted by mixing boron nitride and pyrochlore niobates. The x-ray absorption

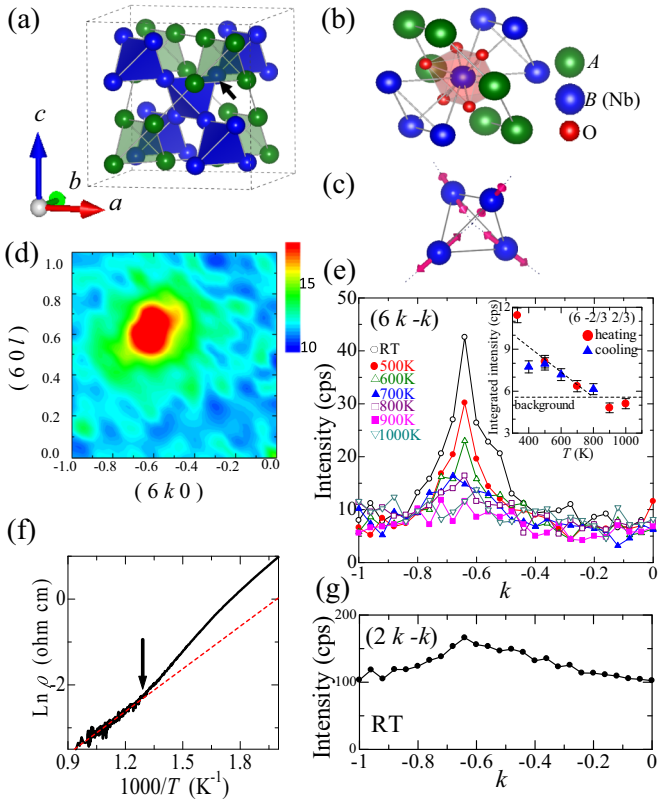

FIG. 1. (a) A (green) and B (Nb) (blue) sublattices in pyrochlore structure $A_2B_2O_7$. (b) Crystal structure around the Nb atom in $A_2Nb_2O_7$. (c) Nb displacement (red arrows) along the [111] direction. (d) Intensity map of the x-ray diffraction with Mo $K\alpha$ radiation in the reciprocal space ($6\ k\ l$) in $A_2Nb_2O_7$ ($A = Nd_{0.5}Ca_{0.5}$). (e) Diffraction intensity in the position ($6\ k\ -k$). Inset: Temperature dependence of integral intensity around ($6\ -2/3\ 2/3$) at $E = 6$ keV. (f) Arrhenius plot in the electrical resistivity. The red dashed line is obtained by the fitting in $T = 800$ K $\sim$ 1000 K. (g) Diffraction intensity in the position ($2\ k\ -k$) at $E = 18.8$ keV.

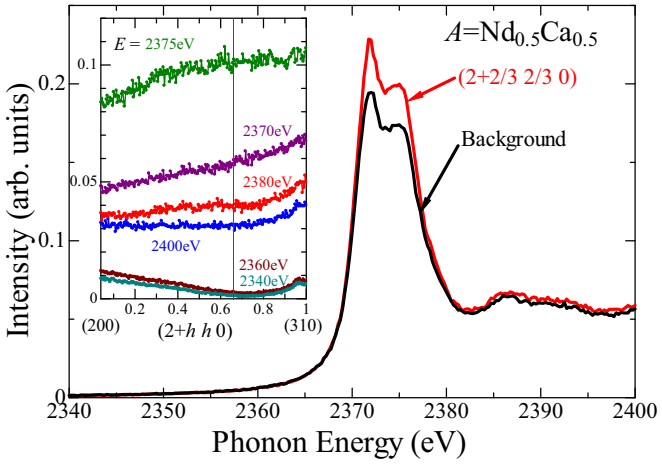

FIG. 2. Photon energy dependence of the diffraction intensity in (2+2/3 2/3 0) (red) and (3 0 0) (black) near the Nb L_3 edge. Inset: Diffraction intensity in (2+h h 0) at various photon energies E. The red vertical line indicates the position of (2+2/3 2/3 0).

function spectroscopy (EXAFS) was analyzed by using the programs ATHENA and ARTEMIS in the Ifeffit library [18].

III. RESULTS

In order to clarify the structure in the title compound, we performed the x-ray diffraction measurements, focusing on the spots in (6 0 0) and (2 0 0), which cannot be seen in an ideal pyrochlore structure owing to the extinction rule in the case of the B-site atomic positions at $x = 0$, 1/4, 1/2, 3/4, and 1. If the B-site atom is displaced from symmetric position, the diffuse scattering should be observed at around (6 0 0) and (2 0 0). In this case, the intensity of the diffuse scattering originating from the Nb displacement around (6 0 0) is expected to be stronger than that around (2 0 0). As shown in Fig. 1(d), the diffuse scattering is seen around ($6\ -2/3\ 2/3$). We also observed the diffuse scattering around ($6\ 2/3\ \pm 2/3$) and ($6\ -2/3\ -2/3$) [10]. We show the x-ray diffuse scattering measured around ($6\ -2/3\ 2/3$) at the higher temperatures in Fig. 1(e). The inset of Fig. 1(e) displays the temperature dependence of the integrated intensities of the diffuse scattering. The diffuse scattering disappears above 800 K. Figure 1(f) displays the resistivity measured in the region $T = 500$–1000 K. The temperature dependence of the resistivity exhibits the activation-type behavior. As indicated by the arrow, an anomaly in the resistivity is observed near $T \simeq 800$ K, which is also where the diffuse scattering disappears. The activation energy of resistivity is $\approx$3400 K above 800 K, and increases up to $\approx$4700 K below 800 K. Thus, this anomaly suggests that the x-ray diffuse scattering is not given merely by the thermal vibration. Figure 1(g) shows the diffuse scattering around ($2\ -2/3\ 2/3$), which corresponds to the diffuse scattering around ($6\ -2/3\ 2/3$).

In order to reveal the contribution of the Nb atoms to the diffuse scattering, we measured the resonant soft x-ray scattering of the Nb L_3 edge, which is sensitive to the difference in the charge and the atomic displacement, as shown in Fig. 2. Since the distance between the reciprocal lattice of (6 0 0) and the origin is larger than the diameter of the Ewald sphere given by the photon energy of the Nb L_3 edge, we measured only around (2 0 0).

The main panel of Fig. 2 shows that the intensity is enhanced as the photon energy approaches the Nb L_3 edge. There was a clear difference in intensity between ($2+2/3\ \ 2/3\ \ 0$) (red curve) and ($3\ \ 0\ \ 0$) (background; black curve) in the energy region between $E = 2370$ and 2376 eV, which suggested a resonant component coming from the Nb atoms. We calculated the atomic scattering factor by using the x-ray absorption spectra measured in the Nb L_3 edge in the pyrochlore oxides including the Nb^{4+}, $Nb^{4.5+}$, and Nb^{5+} ions. The calculated result suggests that the resonant component might contain the effect of the difference in the displacement and the valence between the Nb sites [19]. The region in which the diffuse scattering was measured at $E = 2375$ eV in the inset of Fig. 2 is wider than the diffuse scattering around ($6\ -2/3\ 2/3$) and ($2\ -2/3\ 2/3$) under the off-resonant condition (FWHM of $k \approx 0.17$ and 0.23, respectively). Since the crystal field given by the oxygens around the Nb atom affects only the resonant x-ray diffraction, the difference between the off-resonant x-ray diffraction [Figs. 1(e) and 1(g)] and the resonant x-ray

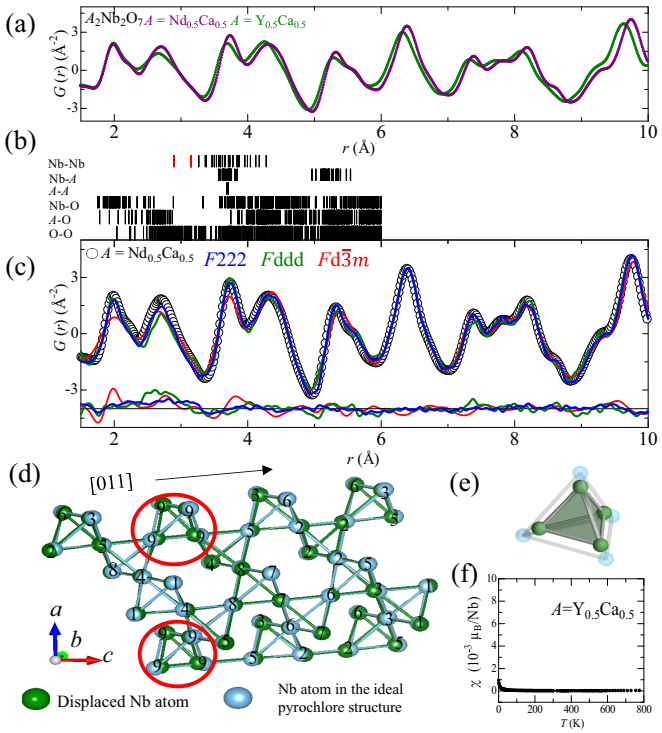

FIG. 3. (a) Neutron PDF in $A = Nd_{0.5}Ca_{0.5}$ (violet) and $Y_{0.5}Ca_{0.5}$ (green). (b) Barcode indicating the distances between the different atom pairs in $A = Nd_{0.5}Ca_{0.5}$. (c) Experimental results (open circle) and the calculated results in $F222$ (blue curve), $Fddd$ (green curve), and $Fd\bar{3}m$ (red curve) of the neutron PDF in $A = Nd_{0.5}Ca_{0.5}$. The R_w value in $Fd\bar{3}m$, $Fddd$, and $F222$ is 18.6%, 17.8%, and 10.9%, respectively. The lower curves indicate the difference between the experimental results and the calculated results. (d) Displaced Nb tetrahedral network in $A = Nd_{0.5}Ca_{0.5}$. The all-in tetrahedron (Nb9) is illustrated within the red circle. The displaced Nb atom positions are determined by the PDF analysis, as listed in Table SI (in the Supplemental Material). Here, the blue and the green spheres indicate the Nb atoms in an ideal pyrochlore structure and the displaced Nb atoms, respectively. (e) All-in type tetrahedron. (f) Magnetic susceptibility in $A = Y_{0.5}Ca_{0.5}$.

diffraction (the inset of Fig. 2) might be due to the crystal field given by the oxygens [20].

Since the x-ray diffuse scattering shows the short-range order and the Nb displacement structure cannot be determined by the conventional refinement (the neutron powder diffraction) [10], we investigated the two-body correlation by the neutron PDF to clarify the local order of the Nb displacement. Figure 3(a) shows the neutron PDF results in $A = Nd_{0.5}Ca_{0.5}$ and $Y_{0.5}Ca_{0.5}$. Both PDF $G(r)$ are similar, indicating the consistency of the Nb displacement parameters in these compounds. Figure 3(c) displays the analysis result of the neutron PDF with the space group $Fd\bar{3}m$ in $A = Nd_{0.5}Ca_{0.5}$. Here, we assumed that the Nb atoms are displaced along the [111] direction [10]. The R_w value in $Fd\bar{3}m$ is rather large (18.6 %) and the analysis results (red curve) do not agree with the experimental results at $r \leqslant 4$ Å. The diffuse scattering position $(6\ -2/3\ 2/3)$ directly indicates that the period of the Nb tetrahedral displacement is $\approx \frac{3}{2}\sqrt{b^2 + c^2} \approx 21$ Å along the [011] direction. Thus, the lattice constants are considered to be multiplied by 3 within the bc plane, that is, $b' \approx c' \approx 31.5$ Å and $a' = 10.34$ Å. Since this crystal system is no longer cubic, we must consider a space group with lower symmetry than the space group $Fd\bar{3}m$. The space group having the highest symmetry in the subgroup of $Fd\bar{3}m$, to which the modulated pyrochlore structure belongs in these lattice constants $(a'\ b'\ c')$, is $F222$ [21]. We therefore performed the PDF analysis under the assumption of $F222$ and these lattice constants. As shown by the blue curve in Fig. 3(c), the results of this analysis ($F222$) were in agreement with the experimental results.

As displayed in Fig. 3(b), the barcodes obtained from the PDF analysis indicate the distances between the different atom pairs in the space group $F222$. We find extremely short distances of the Nb pairs at $r \approx 2.9$ and 3.1 Å, as shown by the red bars in Fig. 3(b). The structural parameters of the Nb atoms in the space group $F222$ in $A = Nd_{0.5}Ca_{0.5}$ are listed in Table S I [22]. Figure 3(d) illustrates the structure of the Nb atoms obtained by the PDF analysis within $r < 10$ Å in $A = Nd_{0.5}Ca_{0.5}$. The Nb atoms are displaced either toward or away from the center of the Nb tetrahedra. There are five types of deformed Nb tetrahedra, including the all-in type deformed tetrahedron ($Nb9_4$) indicated by the red circle in Fig. 3(d) and illustrated in Fig. 3(e). This Nb9 atom shows the largest displacement among the other Nb atoms, and gives the shortest distances of the Nb-Nb pairs [red bars in Fig. 3(b)].

Furthermore, we obtained the XAS near the Nb K edge at room temperature in $A_2Nb_2O_7$ (A = Cd, $Nd_{0.5}Ca_{0.5}$, $Y_{0.5}Ca_{0.5}$). Figure 3(a) displays the results of the Fourier transformation of the EXAFS function $k^3\chi(k)$. The results are plotted as a function of the distances between the x-ray absorption atom (Nb atom) and its surrounding atoms, which are illustrated in Fig. 1(b). The peak intensities at $r \simeq 1.4$ Å and $\simeq 3$ Å reflect the correlations of the Nb-O and the Nb-Nb (Nb-A) atoms, respectively. Since the oxygen atoms are equivalent in the oxygen octahedron in A = Cd with an ideal pyrochlore structure, the distances between Nb and O have a single value in the oxygen octahedron. As shown in Fig. 3(a), the peak intensities at $r \simeq 1.4$ Å in $A = Nd_{0.5}Ca_{0.5}$ and $Y_{0.5}Ca_{0.5}$ are lower than that in A = Cd, indicating that the Nb-O distances are different from the crystal in the former two compounds. While the single peak ($r \simeq 3.3$ Å) is seen in A = Cd in Fig. 3(a), two peaks ($r \simeq 2.7$ and 3.3 Å) are observed in $A = Nd_{0.5}Ca_{0.5}$ and $Y_{0.5}Ca_{0.5}$. The difference in these peak positions suggests a displacement of Nb atoms in the latter two compounds. Figure 3(b) displays the simulation results in $F222$, $Fddd$, and $Fd\bar{3}m$ of the EXAFS in $A = Nd_{0.5}Ca_{0.5}$. In these EXAFS simulations, we used the structural parameters employed in the PDF analysis. The simulation result in the space group $F222$ is consistent with the experimental results of EXAFS.

IV. DISCUSSION

Let us discuss the origin of the Nb displacement [23]. Since the Nb9 atom has the largest displacement, the tetramer of the Nb9 atom plays an important role in the ground state. According to the theoretical study on $Y_2Nb_2O_7$, the Nb pyrochlore lattice consists of the Nb(1) and the Nb(2) atoms [9]. The Nb(2) 4d orbitals are hybridized within a Nb(2) tetrahedron, leading to the Nb(2) displacement toward the

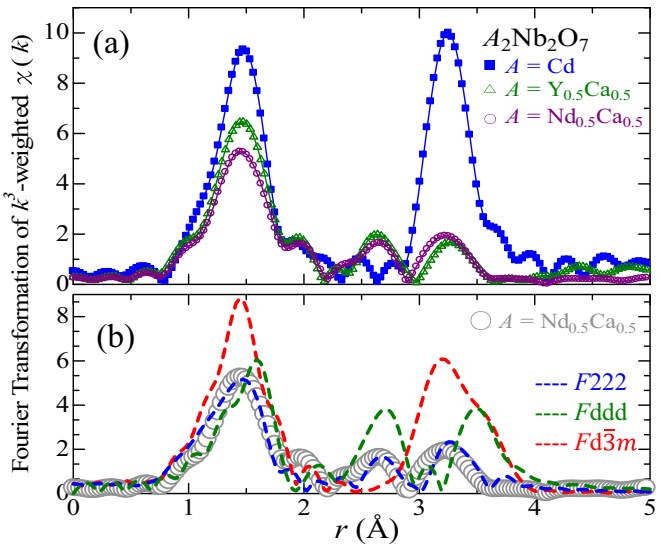

FIG. 4. Fourier transformation of k^3-weighted $\chi(k)$ in A = Cd (blue square), $Y_{0.5}Ca_{0.5}$ (green triangle), and $Nd_{0.5}Ca_{0.5}$ (violet circle) at room temperature. (b) Simulation in $F222$ (blue dashed curve), $Fddd$ (green dashed curve), and $Fd\bar{3}m$ (red dashed curve) and the experimental results (open circle) of the EXAFS in $A = Nd_{0.5}Ca_{0.5}$.

center of the Nb tetrahedra (the all-in type Nb displacement) and the formation of the Nb tetramer. Here, the valence and the displacement δ from an ideal pyrochlore strucutre are +3 and $\delta = 0.45$ Å in the Nb(2) atoms. On the other hand, the Nb(1) atom, whose displacement is smaller than the Nb(2), is not displaced toward the center of the Nb tetrahedra. Since the orbital hybridization (covalency) drives the Nb displacement, the valence of the Nb atoms having a large and small displacement tends to be low and high, respectively [9,24]. The displacement ($\delta \simeq 0.4$) of the Nb9 atom in $A = Nd_{0.5}Ca_{0.5}$ is comparable to that of Nb(2) in A = Y. Therefore, the valences of the Nb9 atom are expected to be lower than the average valence of +4.5, because of the covalency. In the other Nb atoms, the contribution of the covalency is expected to be comparatively small, and the valence is higher. Indeed, in the Nb1 ($\delta \simeq 0.14$ Å), the Nb6 ($\delta \simeq 0.12$ Å), and the Nb7 ($\delta \simeq 0.02$ Å), these valences are estimated at $\simeq +5$ by the bond valence sum in the results of the PDF analysis. The exact value of the Nb valence cannot be determined by the bond valence sum, since the Nb-O bond is a complex structure [6].

In order to compare the electronic energy in the all-in type displacement with an ideal pyrochlore configuration, we performed the band calculation in A = Y. The Fermi energy is located at the band from the Nb 4*d* orbitals in an ideal pyrochlore structure without displacement. According to theoretical study, the all-in type deformed Nb tetrahedra are driven by the hybridization of the Nb 4*d* orbitals [9]. This hybridization reduces the energy of the electron system and opens the energy gap. The produced hybrid orbitals are one hybrid orbital of the four center bond pointing into the center of $Nb(2)_4$ tetrahedra, four hybrid orbitals on the contracted Nb(1) triangles in the $Nb(2)Nb(1)_3$ tetrahedra, and three hybrid orbitals on the faces of the $Nb(2)_4$ tetrahedra. Since the number of the Nb atom is 16 in the unit cell in A = Y, 16 electrons occupy the hybrid orbitals per an all-in type deformed Nb tetrahedron. In $A = Nd_{0.5}Ca_{0.5}$, the experimental results show the 3×3 superstructure in the *bc* plane with the short-range correlation. Four all-in type deformed $Nb9_4$ tetrahedra exist in the superstructure unit cell according to the PDF analysis. The total number of electrons is 72 in the superstructure unit cell, which contains 144 Nb atoms, in $Nb^{4.5+}(4d)^{0.5}$ valence in A $=Nd_{0.5}Ca_{0.5}$. Thus, the 18 electrons can be assigned to each all-in type deformed $Nb9_4$ tetrahedra, which are very close to 16 electrons predicted by the theory in A = Y. The extra two electrons might form an additional all-in type deformed tetrahedra per two supersturucture unit cells, leading to the frustration and the diffuse scattering. As shown in Fig. 2(f), the magnetic susceptibility suggests the non-magnetic state in $A = Y_{0.5}Ca_{0.5}$. In the neutron inelastic scattering of $A = Y_{0.5}Ca_{0.5}$, the magnetic excitation was also not observed in the low energy range. The electrons fully occupy the hybrid orbitals, whose energy is decreased by the all-in type Nb displacement. The resultant gap formation causes the non-magnetic state. This non-magnetic state agrees with the fact that the charge singlet state is non-magnetic in A = Y [8,9].

V. SUMMARY

We investigated the Nb tetrahedral displacement in the pyrochlore niobates. The results of the PDF and the EXAFS analyses revealed the all-in type displacement in the Nb tetrahedra, indicating a non-magnetic charge-disproportionated state. The x-ray diffuse scattering indicates the periodic modulation of the Nb atom and the oxygen octahedra with short correlation lengths.

ACKNOWLEDGMENTS

The authors thank H. Kawamura, R. Kajimoto, Y. Yamasaki, Y. Murakami, and T. Fujikawa for their valuable discussion. This work was partly supported by JSPS KAKENHI Grant No. 24340084 and by the Priority Area "Novel States of Matter Induced by Frustration" (Grant No. 19052003) from MEXT of Japan and by Nippon Sheet Glass Foundation for Materials Science and Engineering. The neutron scattering experiment was approved by the Neutron Science Proposal Review Committee of J-PARC/MLF (Proposal No. 2012B0182) and supported by the Inter-University Research Program on Neutron Scattering of IMSS, KEK. The synchrotron radiation experiments were performed at BL-14B1 of SPring-8 under the Common-User Facility Program of JAEA (Proposal No. 2010A-E02) and under the approval of JASRI (Proposal No. 2010A3614) and at BL-4C of Photon Factory under the approval of the Photon Factory Program Advisory Committee (Proposal No. 2012S2-005).

[1] L. Pauling, J. Am. Chem. Soc. **57**, 2680 (1935).
[2] P. W. Anderson, Phys. Rev. **102**, 1008 (1956).
[3] S. T. Bramwell and M. J. P. Gingras, Science **294**, 1495 (2001).

[4] M. Schmidt, W. Ratcliff, P.G. Radaelli, K. Refson, N. M. Harrison, and S.-W. Cheong, Phys. Rev. Lett. **92**, 056402 (2004).
[5] Y. Horibe, M. Shingu, K. Kurushima, H. Ishibashi, N. Ikeda, K. Kato, Y. Motome, N. Furukawa, S. Mori, and T. Katsufuji, Phys. Rev. Lett. **96**, 086406 (2006).
[6] P. G. Radaelli, Y. Horibe, M. J. Gutmann, H. Ishibashi, C. H. Chen, Richard M. Ibberson, Y. Koyama, Y.-S. Hor, Valery Kiryukhin, and S.-W. Cheong, Nature (London) **416**, 155 (2002).
[7] T. Malcherek, U. Bismayer, and C. Paulmann, J. Phys.: Condens. Matter **22**, 205401 (2010).
[8] H. Fukazawa and Y. Maeno, Phys. Rev. B **67**, 054410 (2003).
[9] P. Blaha, D. J. Singh, and K. Schwarz, Phys. Rev. Lett. **93**, 216403 (2004).
[10] T. M. McQueen, D. V. West, B. Muegge, Q. Huang, K. Noble, H. W. Zandbergen, and R. J. Cava, J. Phys.: Condens. Matter **20**, 235210 (2008).
[11] S. Y. Istomin, O. G. D'yachenko, E. V. Antipov, and G. Svensson, Mater. Res. Bull. **32**, 421 (1997).
[12] H. Iwasaki, S. Sasaki, S. Kishimoto, J. Harada, M. Sakata, Y. Fujii, N. Hamaya, S. Hashimoto, K. Ohshima, and H. Oyanagi, Rev. Sci. Instrum. **60**, 2406 (1989).
[13] Y. Kitajima, J. Electron Spectrosc. Relat. Phenom. **80**, 405 (1996).
[14] H. Nakao, Y. Yamasaki, J. Okamoto, T. Sudayama, Y. Takahashi, K. Kobayashi, R. Kumai, and Y. Murakami, J. Phys.: Conf. Ser. **502**, 012015 (2014).
[15] S. Iikubo, K. Kodama, K. Takenaka, H. Takagi, M. Takigawa, and S. Shamoto, Phys. Rev. Lett. **101**, 205901 (2008).
[16] P. Juhas, T. Davis, C. L. Farrow, and S. J. L. Billinge, J. Appl. Crystallogr. **46**, 560 (2013).
[17] S. Torioge, Y. Ishimoto, N. Hanasaki, Y. Nogami, D. Matsumura, K. Yoshii, Y. Yoneda, and Y. Nishihata, J. Phys.: Conf. Ser. **320**, 012078 (2011).
[18] B. Ravel and M. Newville, J. Synchrotron Radiat. **12**, 537 (2005).
[19] See Supplemental Material at http://link.aps.org/supplemental/10.1103/PhysRevB.93.085109 for calculation of the resonant component in the Nb L_3 edge in the soft x-ray diffraction.
[20] H. Nakao, S. Kodama, K. Kiyoto, Y. Murakami, M. Tsubota, F. Iga, K. Uchihira, T. Takabatake, H. Ohsumi, M. Misumaki, and N. Ikeda, J. Phys. Soc. Jpn. **75**, 094706 (2006).
[21] To examine the symmetry with pyrochlore lattice in the lattice constants b', c', and a', the subgroup of the space group $Fd\bar{3}m$ described in Example 2.18.2.3 in International Table A1 (page 437) is used. Here, the space groups $F4_132$, $F4\bar{3}m$, $Fd\bar{3}$, $F23$, and $R\bar{3}m$ are not reasonable, since these space groups do not have the threefold axis along the [111] direction. The space groups having the first letter I and C are not relevant, since these cannot form a pyrochlore lattice. Therefore, the rest of this subgroup ($Fddd$ and $F222$) are possible candidates.
[22] See Supplemental Material at http://link.aps.org/supplemental/10.1103/PhysRevB.93.085109 for structural parameters of the Nb atoms in the space group $F222$ in $A_2Nb_2O_7$ ($A = Nd_{0.5}Ca_{0.5}$).
[23] We performed the resonant x-ray diffraction measurement near the Nd L_3 edge. Since the resonance signal is not detected near the Nd L_3 edge, we concluded that the diffuse scattering is not caused by the displacement of the A-site atom.
[24] R. E. Cohen, Nature (London) **358**, 136 (1992).